APPLIED OPTICS

Active quantum plasmonics

10.1126/sciadv.1501095

Dana Codruta Marinica,[1] Mario Zapata,[1,2,3] Peter Nordlander,[4] Andrey K. Kazansky,[5,6] Pedro M. Echenique,[5] Javier Aizpurua,[2]* Andrei G. Borisov[1]*

The ability of localized surface plasmons to squeeze light and engineer nanoscale electromagnetic fields through electron-photon coupling at dimensions below the wavelength has turned plasmonics into a driving tool in a variety of technological applications, targeting novel and more efficient optoelectronic processes. In this context, the development of active control of plasmon excitations is a major fundamental and practical challenge. We propose a mechanism for fast and active control of the optical response of metallic nanostructures based on exploiting quantum effects in subnanometric plasmonic gaps. By applying an external dc bias across a narrow gap, a substantial change in the tunneling conductance across the junction can be induced at optical frequencies, which modifies the plasmonic resonances of the system in a reversible manner. We demonstrate the feasibility of the concept using time-dependent density functional theory calculations. Thus, along with two-dimensional structures, metal nanoparticle plasmonics can benefit from the reversibility, fast response time, and versatility of an active control strategy based on applied bias. The proposed electrical manipulation of light using quantum plasmonics establishes a new platform for many practical applications in optoelectronics.

INTRODUCTION

The latest advances in nanofabrication techniques allow for systematic engineering of the plasmonic response of nanostructures, thus offering the possibility of manipulation of light at subwavelength scales (*1*) and its exploitation in numerous applications. Sensors (*2*), nanoantennas (*3*), information transfer (*4*), single photon generation (*5*), enhancement of nonlinear effects (*6*), photochemistry (*7*), heat generation, and hot electron injection (*8*) constitute a subset of research topics related to plasmonics that would strongly benefit from the availability of active mechanisms for controlling the coupling between plasmon excitations and light. Although at present, the plasmon response is mainly tuned during the fabrication process via shape or material control or, alternatively, by the choice of dielectric environment (*9*), it is highly desirable to develop fast, flexible, and reversible procedures for the control of this response. Recent experimental developments have suggested several possibilities for such active control, for instance, using flexible substrates (*10*), liquid crystal environments (*11*), tunable molecular layers (*12*), electrically induced thermal heating (*13*), all-optical modulation using quantum dot arrays (*14*), or excitation of free carriers (*15*). The latter approach allows for ultrafast modulation at femtosecond (10^{-15} s) time scales but requires a pump laser of sufficient power to produce appreciable effects. In this context, electrical control of the plasmonic response via an applied bias, as implemented in two-dimensional (2D) materials (*16*, *17*), appears extremely attractive even though, in that case, this possibility is limited to the terahertz or mid-infrared regime as a result of the low doping concentrations that can be achieved electrically. This strategy also encounters a bottleneck when applied to 3D bulk plasmonic metal nanostructures with high free-electron density, as so far only electrochemistry-based solutions have been proposed (*18*–*20*).

Here, we demonstrate that active electrical control of the plasmonic response of 3D metallic nanostructures at optical frequencies is possible owing to the bias voltage dependence of the electron tunneling conductance across narrow gaps. Indeed, a number of recent experimental (*21*–*25*) and theoretical (*26*–*29*) studies on nanoparticle dimers with subnanometer gaps have demonstrated that electron tunneling through the potential barrier separating two closely spaced nanoparticles can strongly modify the optical response of the system. When electron tunneling is present, the capacitive coupling between the nanoparticles is attenuated, and the corresponding plasmonic modes progressively disappear upon the narrowing of the gap, accompanied by the emergence of new charge transfer plasmon modes (*26*, *27*). In the tunneling regime, the conductance across the junction is the key parameter which defined the optical properties of the dimer, as also discussed in the context of optical rectification in plasmonic nanogaps (*30*, *31*).

So far, the tunneling conductance has been modified by changing the width of the gap (*21*–*24*) or by using plasmonic gaps bridged by self-assembled molecular layers (*25*). However, as used in scanning tunneling microscopy (*32*, *33*), the tunneling barrier between the nanoparticles and thus its effective conductance can also be modified by an applied external bias, as sketched in Fig. 1. This establishes a concept for active and versatile control of the optical response of a 3D metallic nanosystem operating at picosecond time scales, where the latter is determined by the time needed to bias the system.

RESULTS AND DISCUSSION

To demonstrate the proposed bias control of the plasmonic response, we perform a proof-of-principle calculation for two representative systems that show narrow plasmonic gaps: (i) a cylindrical core-shell nanomatryushka (NM) and (ii) a spherical dimer, as illustrated in the insets to Fig. 2 (A and B, respectively). The NM with a geometry (R_1, R_2, R_3) consists of an infinite cylindrical metallic core of radius R_1 and a coaxial

[1]Institut des Sciences Moléculaires d'Orsay, UMR 8214, CNRS, Université Paris Sud, Bâtiment 351, 91405 Orsay Cedex, France. [2]Materials Physics Center, Consejo Superior de Investigaciones Científicas–Universidad del País Vasco/Euskal Herriko Unibertsitatea and Donostia International Physics Center, Paseo Manuel de Lardizabal 5, 20018 Donostia–San Sebastián, Spain. [3]Departamento de Física, Universidad de los Andes, 111711 Bogotá, Colombia. [4]MS61, Laboratory for Nanophotonics, Department of Physics, Rice University, Houston, TX 77005, USA. [5]Donostia International Physics Center, Paseo Manuel de Lardizabal 4, 20018 Donostia–San Sebastián, Spain. [6]IKERBASQUE, Basque Foundation for Science, E-48011 Bilbao, Spain.
*Corresponding author. E-mail: aizpurua@ehu.es (J.A.); andrei.borissov@u-psud.fr (A.G.B.)

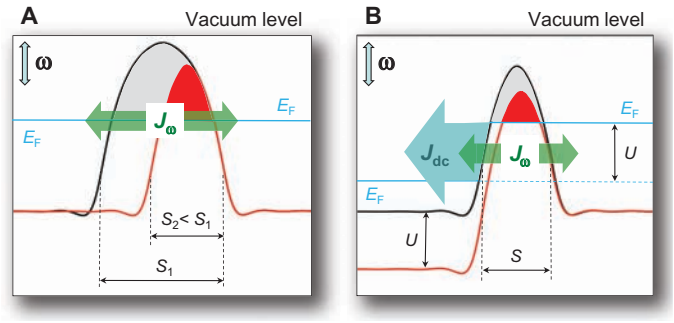

Fig. 1. Schematics of the mechanism underlying the proposed bias-control strategy for active plasmonics. The evolution of the electron tunneling barrier across a nanoparticle junction is shown for two situations. (**A**) The junction width is reduced from S_1 to S_2. The Fermi levels E_F of the left and right leads are aligned. (**B**) A bias U is applied to the left lead, whereas the width of the junction S is kept fixed. The shaded areas represent the tunneling barrier for the electrons at the Fermi energy before (gray) and after (red) the modification of the tunneling barrier, by changing the junction width (A) and the bias (B). The presence of the incident electromagnetic field at frequency ω induces the modulation of one-electron potentials (vertical arrow on the top left corner of the panels). Horizontal green and blue arrows show, respectively, the ac current J_ω due to the optical potential and the dc current J_{dc} due to applied bias U.

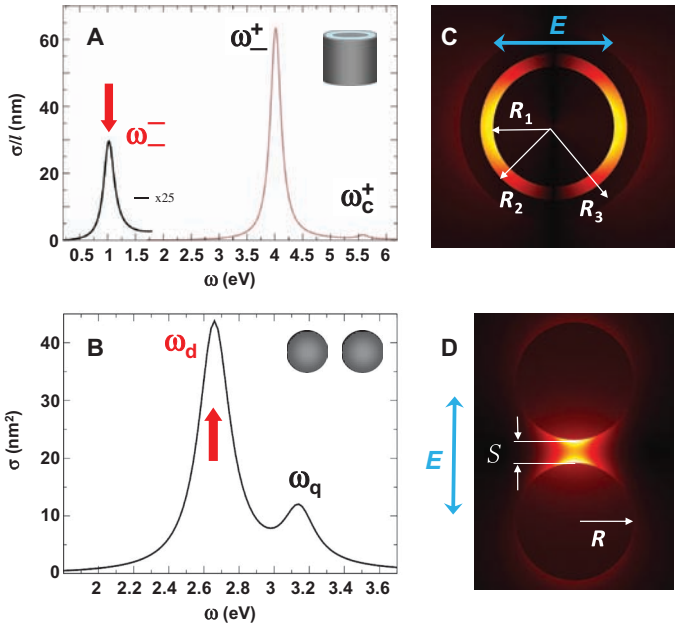

Fig. 2. Optical response of the systems under study. The polarization of the incident light is illustrated with blue arrows. (**A**) The absorption cross section per unit length σ/*l* calculated for a cylindrical core-shell NM (R_1 = 39.2 Å, R_2 = 47.7 Å, R_3 = 61 Å). The NM geometry is given by the radius of the core R_1, the internal radius of the shell R_2, and the external radius of the shell R_3 [see (C)]. The core-shell gap in this case is $S = R_2 - R_1$ = 8.5 Å. The absorption resonances are labeled according to the underlying plasmonic modes (ω^-_-, bonding hybridized plasmon; ω^+_-, resonance with core character; ω^+_c, antibonding mode with shell character). (**B**) The absorption cross section σ for a spherical dimer formed by two spherical nanoparticles with radius R = 21.7 Å, separated by a gap of width S = 8.5 Å. Absorption resonances correspond to the bonding dipolar mode at ω_d and a bonding quadrupolar mode at ω_q. (**C**) The near-field distribution calculated for the ω^-_- plasmon mode of the NM. (**D**) The near-field distribution calculated for the ω_d plasmon mode of the spherical dimer. The most bias-sensitive resonances are marked with red arrows. The calculations consider an electronic density that corresponds to Na metal.

cylindrical metallic shell with internal radius R_2 and external radius R_3. The spherical dimer consists of two identical spherical metallic particles of radius R separated by a narrow gap of width S. Without loss of generality, we assume a vacuum gap for both systems (the possibilities offered by the dielectric filling of the gap will be discussed below). These types of systems are canonical structures that have been widely discussed in the literature. Their plasmonic modes are characterized by the presence of strong localized field enhancements in their gap, as shown in Fig. 2 (C and D). In the case of the NM, we identify the gap mode as the bonding hybridized mode (*34*) ω^-_- associated with the low energy absorption resonance in Fig. 2A (red arrow). In the case of the spherical dimer, the relevant mode is the bonding dipolar plasmon (*26*, *27*) ω_d associated with the main absorption peak in Fig. 2B. In these classical electromagnetic calculations, the quasi-static approximation is adopted, given the small sizes of the systems. The results presented in Fig. 2 are obtained for a gap width S = 8 Å, thus avoiding the effect of tunneling and making it possible to clearly identify the ω^-_- and ω_d modes. However, for narrower gaps, these bonding modes are strongly affected by electron tunneling; thus, they will set the basis for our active control concept. Essentially, as we decrease S, the gap resonances broaden in the optical spectra, and they lose intensity because of resistive losses associated with the tunneling current (*28*, *34*) and short-circuiting of the induced charge distributions at opposite sides of the gap.

To exploit active quantum control with an applied bias based on the sensitivity of the gap resonances (ω^-_- and ω_d) to electron tunneling, we reduce the gap size to $S \approx 6$ Å where tunneling effects, albeit weak, are present. This allows control of the plasmon response by a low external bias (within the electron volt range). In the tunneling regime, the optical response of the systems is obtained from the quantum mechanical calculations within the time-dependent density functional theory (TDDFT) (*35*). In the presence of an external bias, a dc current flows through the gap, a process that represents a real challenge for TDDFT calculations (*36*). We use a strategy where the bias is progressively applied which drives the system into a transitory steady-state regime needed for the calculation of the absorption spectra. More details of our approach are given in the Supplementary Materials. The nanoparticles are described within the jellium model (JM), which describes the optical absorption spectra of a variety of metallic systems, including those of core-shell and spherical dimer nanoparticles (*26*, *27*, *34*). The advantage of the JM is that a full quantum treatment can be performed for sufficiently large systems so that plasmonic modes and steady-state currents are fully developed. We consider nanoparticles made of Na metal, which is a prototype system for the JM. Despite its simplicity, the Na JM robustly captures the main physics and has demonstrated its predictive power in describing tunneling effects on silver and gold plasmonic nanoparticles (*21*–*25*).

Figure 3A shows the absorption spectra calculated with the TDDFT for a cylindrical NM, and Fig. 3B shows the absorption spectra for a spherical dimer. The systems are similar to those used in Fig. 2 but with the width of the tunneling gap reduced to S = 6.4 Å. The incident plane wave is polarized perpendicularly to the symmetry axis in the case of the NM and along the symmetry axis in the case of the spherical dimer.

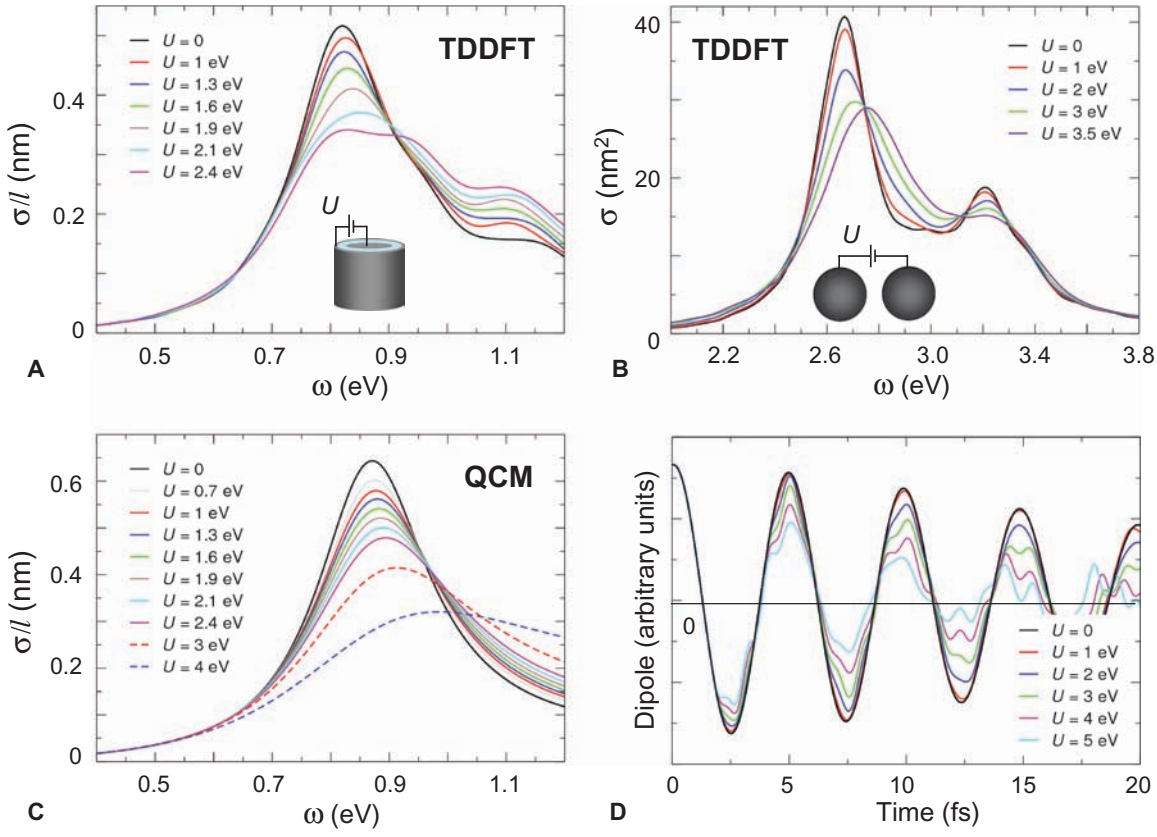

Fig. 3. Effects of applied bias on the plasmonic modes of the NM and the spherical dimer. (**A** and **B**) TDDFT results for the absorption spectra of a cylindrical NM (R_1 = 41.3 Å, R_2 = 47.7 Å, R_3 = 61 Å) and a spherical dimer (R = 21.7 Å) with gap width S = 6.4 Å. (**C**) Absorption cross section per unit length σ/*l* calculated with QCM for the cylindrical NM with the same geometry as in (A). (**D**) Time evolution of the dipole induced in the NM of (A) by an incident pulse of light resonant with the ω_- plasmon mode and polarized perpendicularly to the symmetry axis. The bias is applied at time t = 2 fs. The values of the applied bias are detailed in the insets.

The calculations have been performed for different values of the bias U applied either between the core and the shell of the cylindrical NM or between the nanoparticles forming the dimer, as depicted in the insets to Fig. 3 (A and B). Remarkably, application of the bias produces significant changes in the absorption spectra. In particular, a considerable decrease in the resonance absorption peak is apparent. Within the studied bias range $0 < U < 3$ eV, we calculate an ≈30% variation of the maximum of the absorption cross section primarily because of the broadening of the plasmon resonance. Thus, even a moderate change in the dc bias results in a significant modulation of the plasmon response. It is worth mentioning that the (bias-dependent) coupling of the collective plasmon modes with single-particle electron-hole excitations, which is behind the plasmon mode decay, leads to the features in the absorption spectra, as observed in the case of NMs shown in Fig. 3A (*29*, *37*).

To understand the TDDFT results, let us consider a junction between two flat metal surfaces separated by a narrow gap of width S. Within a linear response, the presence of the optical field E_ω at frequency ω induces a tunneling current at the same frequency. The dissipative component (in phase with the driving field) of this current density can be expressed (in atomic units) as (*38*)

$$J_\omega(U,V_\omega) = V_\omega/(2\omega)[J_{dc}(U+\omega) - J_{dc}(U-\omega)] \quad (1)$$

where U is the applied dc bias, $V_\omega \approx SE_\omega$ is the (small) optical bias across the junction, and $J_{dc}(U \pm \omega)$ is the dc current at bias $U \pm \omega$. For a slow variation of J_{dc} with U, we obtain the classical limit

$$J_\omega(U,V_\omega) = S(dJ_{dc}/dU)E_\omega \quad (2)$$

An increase in the applied bias at a fixed gap width S leads to a lower tunneling barrier; thus, the conductivity $\sigma(U,S) = S(dJ_{dc}/dU)$ becomes larger, resulting in a larger tunneling current at optical frequency J_ω. Similar to the cases where the gap width S is reduced (*26*–*29*) (at zero bias), the existence of a larger tunneling current at optical frequency results in a quenching of the bonding plasmon peak in the absorption spectrum. This is a consequence of the partial neutralization of the screening charges at opposite sides of the junction, resulting in increased resistive losses. For the gap resonance of the spherical dimer (Fig. 3B), the peak blue shifts with increasing U, consistent with the reduction of the capacitive coupling across the gap, which results in a screened bonding dimer plasmon. The evolution of the absorption spectra of the spherical dimer with the applied bias is similar to earlier theoretical results obtained by varying the conductance across the junction (*39*), which further supports our interpretation of the results. For a larger gap width S, the tunneling probability decreases so that a larger applied bias U is needed to induce the same tunneling current and thus a similar degree of plasmon response modification (Supplementary Materials).

To further confirm that the effect of the bias tuning of the plasmon resonances is mainly due to tunneling, we also calculate the optical response of the cylindrical NM using the quantum corrected model (QCM) (*28*). The QCM allows for inclusion of quantum tunneling effects within the framework of classical Maxwell's equations. To this end, the optical response of the gap is described by a local effective dielectric function

$$\varepsilon_g(U,S) = 1 + i4\pi\sigma_g(U,S)/\omega \quad (3)$$

The bias-dependent conductivity $\sigma_g(U,S)$ accounts for the tunneling current at optical frequencies and finite bias. The advantage of performing the QCM calculations for NM is that because of the fixed size of the vacuum gap, the corresponding $\sigma_g(U,S)$ in this case can be directly deduced from the TDDFT calculations without any parameters. Thus, the "quantum" relationship between the tunneling current and the field in the gap is reproduced (Supplementary Materials). The QCM results shown in Fig. 3C correctly capture all the main spectral trends as a function of bias variation, as observed when compared with the full quantum TDDFT calculations (Fig. 3A). This suggests that the bias-induced variation of the conductivity across the junction is indeed at the origin of the spectral changes obtained with the TDDFT calculations. Furthermore, the QCM approach allows calculations for larger bias values, where the TDDFT would be difficult to implement. The results for such a large bias are shown with dashed lines in Fig. 3C. For $U \approx 4$ eV, the absorption cross section is decreased by more than a factor of 2 at the resonance frequency, and the plasmon resonance is nearly quenched.

The dependence of the absorption spectra on the applied bias reflects the modification of the plasmon dynamics in the system. In particular, the increasing width of the resonance peaks in the absorption spectra indicates faster damping of the underlying plasmon modes. We illustrate this connection between energy (ω)–resolved and temporal properties of the system in Fig. 3D, where we show the time evolution of the dipole induced in the cylindrical NM by an external electromagnetic pulse with a duration of 20 fs. The pulse has a Gaussian envelope and a carrier frequency resonant with the gap plasmon. After the termination of the pulse (reference time $t = 0$), the time evolution of the induced dipole is given by its decaying oscillations at the plasmon frequency ω_-, as shown in Fig. 3D. We compare the dipole dynamics when no bias is applied (black line) with the situation when the bias between the core and the shell is suddenly switched "on" at a time $t = 2$ fs. The sudden perturbation of the system leads to the weak excitation of the higher-energy ω_+ resonance with core character and of the ω_c^+ antibonding mode with shell character. These appear as high-frequency modulations of the main signal, given by the time evolution of the dipole associated with the bonding plasmon ω_-, which is the target of the sought electrical control. An applied bias results in a faster decay and dephasing of the plasmon as a result of the increase in electron tunneling. The larger the applied bias, the stronger the effect is. This result is the time domain equivalent to the broadening of the absorption peaks observed in the frequency domain in Fig. 3 (A to C).

SUMMARY AND CONCLUSIONS

In summary, we have proposed a novel strategy for active control of junction plasmon resonances based on the application of a bias across the gap. The physical origin of the effect is a bias-induced change in the electron tunneling barrier, which in turn controls the conductive coupling between the two nanostructures. The feasibility of the approach has been demonstrated with proof-of-principle calculations based on the quantum mechanical TDDFT. Although we here considered vacuum gaps, filling the plasmonic gap with dielectric materials such as oxides will also modify the tunneling barrier. This effect may be useful for practical realizations of the proposed device because it introduces additional tuning modalities. Thus, the lowering of the tunneling barrier offers the possibility of reaching the sought control for broader gaps. Further extensions of this concept may include molecular linkers with conductance windows allowing for on/off switch functionalities.

Quantum active control of plasmons, as demonstrated here, is inherently a fast (picosecond) process allowing operation at the time scales of modern electronics and reversible and progressive tuning of the plasmon resonances. This opens appealing perspectives for the development of tunable absorbers for solar energy harvesting, control of information transfer in plasmonic waveguides, and manipulation of plasmon-exciton couplings. Our concept of electrical control of light in metallic nanostructures thus provides a new platform for many practical applications in photonics and optoelectronics.

MATERIALS AND METHODS

The calculations of the linear response of the plasmonic systems presented here are based on the Kohn-Sham (K-S) scheme of the TDDFT (*35*), which allows us to treat the quantum dynamics of the many-electron system, triggered by an external perturbation such as an optical pulse. The time-dependent electron density at a given position $\vec{r}$ is given by

$$n(\vec{r},t) = \Sigma_{occ}|\psi_j(\vec{r},t)|^2$$

where the sum runs over all occupied (occ) K-S orbitals $\psi_j(\vec{r},t)$. The time evolution of K-S orbitals is given by the time-dependent Schrödinger equation (we use atomic units in this section unless otherwise stated)

$$i\frac{\partial\psi_j(\vec{r},t)}{\partial t} = \left(T + V_{eff}[n](\vec{r},t)\right)\psi_j(\vec{r},t) \quad (4)$$

where $T = -\frac{1}{2}\Delta$ is the kinetic energy operator and $V_{eff}[n](\vec{r},t)$ is the effective K-S potential that depends on the electron density. The effective K-S potential is given by the sum of the Hartree potential V_H, the exchange correlation potential V_{xc}, and the external potential V_{ext} as

$$V_{eff}[n](\vec{r},t) = V_H[n](\vec{r},t) + V_{xc}[n](\vec{r},t) + V_{ext}(\vec{r},t) \quad (5)$$

The Hartree potential is calculated within a nonretarded approximation, which is fully justified in our case when considering the polarization of the electric field and the small radii of the NM and the spherical dimer. For the exchange correlation potential, we use the adiabatic local density approximation (*35*, *40*–*42*) with the exchange correlation kernel of Gunnarsson and Lundqvist (*43*). The external potential allows us to simulate the effect of the applied external bias and also represents the incident electromagnetic "probe" pulse. Once the time-dependent response of the system to the electromagnetic "probe" pulse is calculated, the Fourier time-to-frequency transform yields the frequency-resolved quantities of interest. Thus, the optical absorption cross section is given by

$$\sigma(\omega) = \frac{4\pi\omega}{c}\mathrm{Im}\{\alpha(\omega)\}$$

where c is the speed of light in vacuum and $\alpha(\omega)$ is the dipolar polarizability of the system.

The metal nanoparticles are treated within the spherical JM approximation (*26*, *27*, *34*) so that the full quantum TDDFT studies can handle model systems comprising a sufficiently large number of conduction electrons with well-developed plasmonic modes. The details of the atomistic structure are neglected within the JM, and the ionic cores of the atoms are represented by a uniform background charge density $n_+ = \left(\frac{4\pi}{3} r_s^3\right)^{-1}$ contained within the volume defined by the jellium edges (metal surfaces). The Wigner-Seitz radius r_s is set equal to $4a_0$ (Bohr radius a_0 = 0.53 Å), corresponding to the Na metal that is a prototype system for the JM description. The cylindrical NM and the spherical dimer have a cylindrical symmetry such that we can address up to 300 conduction electrons per 1-Å length in the former case and 1074 electrons per nanoparticle in the latter case.

The QCM (*28*) calculations in our study are implemented to support the interpretation of the TDDFT results. Because the essential physics contained in the QCM is associated with the presence of tunneling across the junctions, the comparison of the two approaches (TDDFT and QCM) for the NM clearly confirms that the bias effect on the plasmon resonances is due to tunneling. In the QCM, the metal nanoparticles are described with the use of a Drude dielectric function

$$\varepsilon(\omega) = 1 - \frac{\omega_p^2}{\omega(\omega + i\eta)} \quad (6)$$

where the attenuation and the plasma frequency are, respectively, η = 0.218 eV and ω_p = 5.16 eV. This choice of parameters allows us to account for electron spill-out effects and plasmon line broadening as a consequence of the decay of plasmons into electron-hole one-particle excitations (*44*). The vacuum gap between the core and the shell of the cylindrical NM is filled with an effective material characterized by the dielectric function given by Eq. 3 to capture the effect of the electron tunneling. The tunneling conductivity across a gap with width S at an applied dc bias U is obtained from the TDDFT calculations as

$$\sigma_g(U,S) = S\frac{dJ_{dc}(U,S)}{dU} \quad (7)$$

Here, $J_{dc}(U,S)$ represents the dc tunneling current density through the middle of the gap calculated with the TDDFT at the steady-state regime reached for the bias U between the core and the shell in the case of a NM gap (for further details, see Supplementary Materials). Classical electromagnetic calculations within the quasi-static approximation, using the model dielectric function given by Eqs. 6 and 7, reproduce the absorption spectra calculated with the TDDFT for the individual cylindrical nanowire of radius R = 61 Å, as well as the applied bias dependence of the absorption spectra calculated with the TDDFT for the cylindrical NM.

SUPPLEMENTARY MATERIALS

Supplementary material for this article is available at http://advances.sciencemag.org/cgi/content/full/1/11/e1501095/DC1

Details of quantum mechanical calculations within the TDDFT

Fig. S1. Effective one-electron potential (A) and ground-state electron density (B) calculated with density functional theory for the cylindrical NMs with different gap sizes.

Fig. S2. Frequency-dependent absorption cross section per unit length calculated with the TDDFT for the infinite cylinder with radius R = 61 Å.

Fig. S3. Dependence of the absorption spectra of the cylindrical NM (A) and spherical dimer (B) on the size of the plasmonic gap.

Fig. S4. Effective one-electron potentials (A) and Hartree and exchange-correlation contributions to the one-electron potentials (B) calculated with density functional theory for cylindrical NM (R_1 = 41.3 Å, R_2 = 47.7 Å, R_3 = 61 Å) with a bias applied between the core and the shell.

Fig. S5. (A to D) Electron dynamics triggered by the bias applied between the core and the shell of the cylindrical NM (R_1 = 41.3 Å, R_2 = 47.7 Å, R_3 = 61 Å).

Fig. S6. Applied bias dependence of the absorption cross section per unit length calculated for the cylindrical NM (R_1 = 41.3 Å, R_2 = 47.7 Å, R_3 = 61 Å) using the TDDFT (A and B) and QCM (C) approaches within the frequency range corresponding to the bonding hybridized plasmon mode.

Fig. S7. Applied bias dependence of the absorption cross section per unit length calculated with the TDDFT for the cylindrical NM within the frequency range corresponding to the plasmon mode with core character.

Fig. S8. Time evolution of the effective bias triggered by the slowly varying external potential applied to the spherical dimer.

Fig. S9. Time evolution of the induced dipole (A) and the effective bias (B) calculated with the TDDFT for the cylindrical NM in response to the illumination by the "probe" pulse and sudden change in the applied bias.

Fig. S10. Current-voltage characteristic of the cylindrical NM (R_1 = 41.3 Å, R_2 = 47.7 Å, R_3 = 61 Å). Additional calculations for different sizes of gap S

Fig. S11. Applied bias dependence of the absorption cross section per unit length calculated with the TDDFT for the cylindrical NM (R_1 = 40.3 Å, R_2 = 47.7 Å, R_3 = 61 Å).

Fig. S12. (A and B) TDDFT calculations for the spherical dimer with a gap of S = 5 Å.

References (*45*–*61*)

REFERENCES AND NOTES

1. J. A. Schuller, E. S. Barnard, W. Cai, Y. C. Jun, J. S. White, M. L. Brongersma, Plasmonics for extreme light concentration and manipulation. *Nat. Mater.* **9**, 193–204 (2010).
2. J. N. Anker, W. P. Hall, O. Lyandres, N. C. Shah, J. Zhao, R. P. Van Duyne, Biosensing with plasmonic nanosensors. *Nat. Mater.* **7**, 442–453 (2008).
3. P. Mühlschlegel, H. J. Eisler, O. J. Martin, B. Hecht, D. W. Pohl, Resonant optical antennas. *Science* **308**, 1607–1609 (2005).
4. D. K. Gramotnev, S. I. Bozhevolnyi, Plasmonics beyond the diffraction limit. *Nat. Photonics* **4**, 83–91 (2010).
5. A. V. Akimov, A. Mukherjee, C. L. Yu, D. E. Chang, A. S. Zibrov, P. R. Hemmer, H. Park, M. D. Lukin, Generation of single optical plasmons in metallic nanowires coupled to quantum dots. *Nature* **450**, 402–406 (2007).
6. M. Kauranen, A. V. Zayats, Nonlinear plasmonics *Nat. Photonics* **6**, 737–748 (2012).
7. G. Baffou R. Quidant, Nanoplasmonics for chemistry. *Chem. Soc. Rev.* **43**, 3898–3907 (2014).
8. C. Clavero, Plasmon-induced hot-electron generation at nanoparticle/metal-oxide interfaces for photovoltaic and photocatalytic devices. *Nat. Photonics* **8**, 95–103 (2014).
9. N. C. Lindquist, P. Nagpal, K. M. McPeak, D. J. Norris, S.-H. Oh, Engineering metallic nanostructures for plasmonics and nanophotonics. *Rep. Prog. Phys.* **75**, 036501 (2012).
10. S. Aksu, M. Huang, A. Artar, A. A. Yanik, S. Selvarasah, M. R. Dokmeci, H. Altug, Flexible plasmonics on unconventional and nonplanar substrates. *Adv. Mater.* **23**, 4422–4430 (2011).
11. O. Buchnev, J. Y. Ou, M. Kaczmarek, N. I. Zheludev, V. A. Fedotov, Electro-optical control in a plasmonic metamaterial hybridised with a liquid-crystal cell. *Opt. Express* **21**, 1633–1638 (2013).
12. Y. B. Zheng, Y.-W. Yang, L. Jensen, L. Fang, B. K. Juluri, A. H. Flood, P. S. Weiss, J. F. Stoddart, T. J. Huang, Active molecular plasmonics: Controlling plasmon resonances with molecular switches. *Nano Lett.* **9**, 819–825 (2009).
13. T. Nikolajsen, K. Leosson, S. I. Bozhevolnyi, Surface plasmon polariton based modulators and switches operating at telecom wavelengths. *Appl. Phys. Lett.* **85**, 5833–5835 (2004).
14. D. Pacifici, H. J. Lezec, H. A. Atwater, All-optical modulation by plasmonic excitation of CdSe quantum dots. *Nat. Photonics* **1**, 402–406 (2007).
15. K. F. MacDonald, Z. L. Sámson, M. I. Stockman, N. I. Zheludev, Ultrafast active plasmonics. *Nat. Photonics* **3**, 55–58 (2009).
16. F. H. L. Koppens, D. E. Chang, F. J. García de Abajo, Graphene plasmonics: A platform for strong light–matter interactions. *Nano Lett.* **11**, 3370–3377 (2011).
17. A. N. Grigorenko, M. Polini, K. S. Novoselov, Graphene plasmonics. *Nat. Photonics* **6**, 749–758 (2012).
18. L.-H. Shao, M. Ruther, S. Linden, S. Essig, K. Busch, J. Weissmüller, M. Wegener, Electrochemical modulation of photonic metamaterials. *Adv. Mater.* **22**, 5173–5177 (2010).
19. S. K. Dondapati, M. Ludemann, R. Müller, S. Schwieger, A. Schwemer, B. Händel, D. Kwiatkowski, M. Djiango, E. Runge, T. A. Klar, Voltage-induced adsorbate damping of single gold nanorod plasmons in aqueous solution. *Nano Lett.* **12**, 1247–1252 (2012).
20. C. Novo, A. M. Funston, A. K. Gooding, P. Mulvaney, Electrochemical charging of single gold nanorods. *J. Am. Chem. Soc.* **131**, 14664–14666 (2009).

21. K. J. Savage, M. M. Hawkeye, R. Esteban, A. G. Borisov, J. Aizpurua, J. J. Baumberg, Revealing the quantum regime in tunnelling plasmonics. *Nature* **491**, 574–577 (2012).
22. J. A. Scholl, A. García-Etxarri, A. L. Koh, J. A. Dionne, Observation of quantum tunneling between two plasmonic nanoparticles. *Nano Lett.* **13**, 564–569 (2013).
23. G. Hajisalem, M. S. Nezami, R. Gordon, Probing the quantum tunneling limit of plasmonic enhancement by third harmonic generation. *Nano Lett.* **14**, 6651–6654 (2014).
24. W. Zhu, K. B. Crozier, Quantum mechanical limit to plasmonic enhancement as observed by surface-enhanced Raman scattering. *Nat. Commun.* **5**, 5228 (2014).
25. S. F. Tan, L. Wu, J. K. Yang, P. Bai, M. Bosman, C. A. Nijhuis, Quantum plasmon resonances controlled by molecular tunnel junctions. *Science* **343**, 1496–1499 (2014).
26. J. Zuloaga, E. Prodan, P. Nordlander, Quantum description of the plasmon resonances of a nanoparticle dimer. *Nano Lett.* **9**, 887–891 (2009).
27. D. C. Marinica, A. K. Kazansky, P. Nordlander, J. Aizpurua, A. G. Borisov, Quantum plasmonics: Nonlinear effects in the field enhancement of a plasmonic nanoparticle dimer. *Nano Lett.* **12**, 1333–1339 (2012).
28. R. Esteban, A. G. Borisov, P. Nordlander, J. Aizpurua, Bridging quantum and classical plasmonics with a quantum-corrected model. *Nat. Commun.* **3**, 825 (2012).
29. L. Stella, P. Zhang, F. J. García-Vidal, A. Rubio, P. García-González, Performance of nonlocal optics when applied to plasmonic nanostructures. *J. Phys. Chem. C* **117**, 8941–8949 (2013).
30. D. R. Ward, F. Hüser, F. Pauly, J. C. Cuevas, D. Natelson, Optical rectification and field enhancement in a plasmonic nanogap. *Nat. Nanotechnol.* **5**, 732–736 (2010).
31. A. Stolz, J. Berthelot, M.-M. Mennemanteuil, G. Colas des Francs, L. Markey, V. Meunier, A. Bouhelier, Nonlinear photon-assisted tunneling transport in optical gap antennas. *Nano Lett.* **14**, 2330–2338 (2014).
32. J. G. Simmons, Generalized formula for the electric tunnel effect between similar electrodes separated by a thin insulating film. *J. Appl. Phys.* **34**, 1793–1803 (1963).
33. A. Garcia-Lekue, D. Sanchez-Portal, A. Arnau, L. W. Wang, Plane-wave based electron tunneling through field emission resonance states. *Phys. Rev. B* **88**, 155441 (2013).
34. V. Kulkarni, E. Prodan, P. Nordlander, Quantum plasmonics: Optical properties of a nanomatryushka. *Nano Lett.* **13**, 5873–5879 (2013).
35. M. A. L. Marques, E. K. U. Gross, Time-dependent density functional theory. *Annu. Rev. Phys. Chem.* **55**, 427–455 (2004).
36. S. Kurth, in *Fundamentals of Time-Dependent Density Functional Theory, Lecture Notes in Physics*, M. A. L. Marques, N. Maitra, F. Nogueira, E. K. U. Gross, A. Rubio, Eds. (Springer, Berlin, 2012).
37. E. Prodan, P. Nordlander, N. J. Halas, Effects of dielectric screening on the optical properties of metallic nanoshells. *Chem. Phys. Lett.* **368**, 94–101 (2003).
38. J. R. Tucker, M. J. Feldman, Quantum detection at millimeter wavelengths. *Rev. Mod. Phys.* **57**, 1055–1113 (1985).
39. O. Pérez-González, N. Zabala, A. G. Borisov, N. J. Halas, P. Nordlander, J. Aizpurua, Optical spectroscopy of conductive junctions in plasmonic cavities. *Nano Lett.* **10**, 3090–3095 (2010).
40. M. E. Casida, Time-dependent density-functional theory for molecules and molecular solids. *J. Mol. Struct. Theochem*. **914**, 3–18 (2009).
41. Th. Fennel, K.-H. Meiwes-Broer, J. Tiggesbäumker, P.-G. Reinhard, P. M. Dinh, E. Suraud, Laser-driven nonlinear cluster dynamics. *Rev. Mod. Phys.* **82**, 1793–1842 (2010).
42. K. Burke, J. Werschnik, E. K. U. Gross, Time-dependent density functional theory: Past, present, and future. *J. Chem. Phys.* **123**, 062206 (2005).
43. O. Gunnarsson, B. I. Lundqvist, Exchange and correlation in atoms, molecules, and solids by the spin-density-functional formalism. *Phys. Rev. B* **13**, 4274 (1976).
44. J. Lermé, Size evolution of the surface plasmon resonance damping in silver nanoparticles: Confinement and dielectric effects. *J. Phys. Chem. C* **115**, 14098–14110 (2011).
45. M. Quijada, A. G. Borisov, I. Nagy, R. Díez Muiño, P. M. Echenique, Time-dependent density-functional calculation of the stopping power for protons and antiprotons in metals. *Phys. Rev. A* **75**, 042902 (2007).
46. T. V. Teperik, P. Nordlander, J. Aizpurua, A. G. Borisov, Quantum effects and nonlocality in strongly coupled plasmonic nanowire dimers. *Opt. Express* **21**, 27306–27325 (2013).
47. A. G. Borisov, J. P. Gauyacq, S. V. Shabanov, Wave packet propagation study of the charge transfer interaction in the F^-–Cu(1 1 1) and –Ag(1 1 1) systems. *Surf. Sci.* **487**, 243–257 (2001).
48. E. V. Chulkov, A. G. Borisov, J. P. Gauyacq, D. Sánchez-Portal, V. M. Silkin, V. P. Zhukov, P. M. Echenique, Electronic excitations in metals and at metal surfaces. *Chem. Rev.* **106**, 4160–4206 (2006).
49. D. Neuhauser, M. Baer, The time-dependent Schrödinger equation: Application of absorbing boundary conditions. *J. Chem. Phys.* **90**, 4351 (1989).
50. P. Zhang, J. Feist, A. Rubio, P. García-González, F. J. García-Vidal, *Ab initio* nanoplasmonics: The impact of atomic structure. *Phys. Rev. B* **90**, 161407(R) (2014).
51. M. Barbry, P. Koval, F. Marchesin, R. Esteban, A. G. Borisov, J. Aizpurua, D. Sánchez-Portal, Atomistic near-field nanoplasmonics: Reaching atomic-scale resolution in nanooptics. *Nano Lett.* **15**, 3410–3419 (2015).
52. T. Reiners, C. Ellert, M. Schmidt, H. Haberland, Size dependence of the optical response of spherical sodium clusters. *Phys. Rev. Lett.* **74**, 1558 (1995).
53. R. C. Monreal, T. J. Antosiewicz, S. P. Apell, Competition between surface screening and size quantization for surface plasmons in nanoparticles. *New J. Phys.* **15**, 083044 (2013).
54. J. M. Pitarke, F. Flores, P. M. Echenique, Tunneling spectroscopy: Surface geometry and interface potential effects. *Surf. Sci.* **234**, 1–16 (1990).
55. R. Baer, T. Seideman, S. Ilani, D. Neuhauser, *Ab initio* study of the alternating current impedance of a molecular junction. *J. Chem. Phys.* **120**, 3387–3396 (2004).
56. M. Cini, Time-dependent approach to electron transport through junctions: General theory and simple applications. *Phys. Rev. B* **22**, 5887–5899 (1980).
57. J. S. Evans, T. Van Voorhis, Dynamic current suppression and gate voltage response in metal–molecule–metal junctions. *Nano Lett.* **9**, 2671–2675 (2009).
58. R. Esteban, A. Zugarramurdi, P. Zhang, P. Nordlander, F. J. García-Vidal, A. G. Borisov, J. Aizpurua, A classical treatment of optical tunneling in plasmonic gaps: Extending the quantum corrected model to practical situations. *Faraday Discuss.* **178**, 151–183 (2015).
59. M. H. Pedersen, M. Büttiker, Scattering theory of photon-assisted electron transport. *Phys. Rev. B* **58**, 12993 (1998).
60. K. Kaasbjerg, A. Nitzan, Theory of light emission from quantum noise in plasmonic contacts: Above-threshold emission from higher-order electron-plasmon scattering. *Phys. Rev. Lett.* **114**, 126803 (2015).
61. M. Zapata, Á. S. Camacho Beltrán, A. G. Borisov, J. Aizpurua, Quantum effects in the optical response of extended plasmonic gaps: Validation of the quantum corrected model in core-shell nanomatryushkas. *Opt. Express* **23**, 8134–8149 (2015).

Acknowledgments: D.C.M. and A.G.B. gratefully acknowledge the hospitality of the Donostia International Physics Center. **Funding:** J.A. acknowledges support from the Spanish Ministry of Economy and Competitiveness through projects FIS2013-41184-P and 2015CD0010 of the Consejo Superior de Investigaciones Científicas scientific cooperation program for development "I-COOP LIGHT" 2015. P.N. acknowledges support from the Robert A. Welch Foundation (grant C-1222) and the Air Force Office of Science and Research (grant FA9550-15-1-0022). M.Z. acknowledges financial support from the Departamento Administrativo de Ciencia, Tecnología e Innovación–COLCIENCIAS and Facultad de Ciencias from Universidad de los Andes. **Author contributions:** A.G.B., A.K.K., P.N., and J.A. conceptualized the control of the optical response of a junction by manipulating the tunneling barrier with an external dc bias. M.Z., D.C.M., and A.G.B. developed the TDDFT and QCM calculations of the optical response. A.G.B., J.A., and P.N. wrote the main parts of the manuscript. All authors discussed the effects and results and suggested ways to improve and more clearly reveal the active strategy of control. **Competing interests:** The authors declare that they have no competing interests. **Data and materials availability:** All data used to obtain the conclusions in this paper are available in [cite the publicly available repository] or presented in the paper and/or the Supplementary Materials.

Submitted 13 August 2015
Accepted 23 October 2015
Published 18 December 2015
10.1126/sciadv.1501095

Citation: D. C. Marinica, M. Zapata, P. Nordlander, A. K. Kazansky, P. M. Echenique, J. Aizpurua, A. G. Borisov, Active quantum plasmonics. *Sci. Adv.* **1**, e1501095 (2015).